Volume holographic data storage at an areal density of 250 gigapixels/in.^{2}

Geoffrey W. Burr, C. Michael Jefferson, Hans Coufal, Mark Jurich, John A. Hoffnagle, Roger M. Macfarlane, and Robert M. Shelby

IBM Almaden Research Center, 650 Harry Road, San Jose, California 95120

Received September 20, 2000

One thousand volume holographic data pages, each containing 1×10^6 pixels, are stored in a common volume of $LiNbO_3$:Fe by use of the 90° geometry. An effective transverse aperture of 1.6 mm × 1.6 mm, realized by repetition of this experiment at each of the eight surrounding locations, results in a demonstrated areal density of 394 pixels/μm^2 (254 Gpixels/in.^{2}). Short-focal-length Fourier optics provide a tightly confined object beam at the crystal; the reference beam is angle multiplexed. Data pages retrieved with a 1024 × 1024 CCD camera are processed to remap bad spatial light modulator pixels and to compensate for global and local pixel misregistration and are then decoded with a strong 8-bits-from-12-pixels modulation code. The worst-case raw bit-error rate (BER) before error correction was 1.1×10^{-3}, sufficient to deliver a user BER of 10^{-12} at an overall code rate of 0.61 user bits per detector pixel. This result corresponds to 1.08% of the well-known theoretical volumetric density limit of $1/\lambda^3$.

OCIS code: 210.2860.

One of the long-standing attractions of volume holographic data storage has always been the potential for storing data at a volumetric density of $1/\lambda^3$, where λ is the wavelength of light.[1] In storage of data with holograms, input data pages of bright and dark pixels enter a storage volume through an aperture, A, and the optical interference pattern between this object beam and a coherent reference beam is recorded throughout the thickness, L. The Bragg-selective properties of volume holograms allow independent recall of any data page. The $1/\lambda^3$ theoretical density limit would be reached by multiplexing of L/λ data pages, each containing A/λ^2 bits of data, within the same volume $V = AL$. High capacity is then realized by arrangement of multiple storage volumes with contiguous input apertures and a common thickness. Examples include rotating disks of thickness L (Ref. 2) and nonmechanical steering of the object beam to locations distributed across the face of a large crystal.[3] In this context, it is useful to discuss the areal density of holographic data storage: the amount of data in each storage volume divided by the aperture, A.

As aperture A shrinks, areal density increases, but at the cost of increased interpixel cross talk. Ideally, light from a particular input spatial light modulator (SLM) pixel should arrive at only the corresponding detector pixel. However, diffraction causes the image transmitted through aperture A, and thus the holographic reconstruction, to be spatially blurred. Given the focal length of the imaging lens, f, and the spacing between SLM pixels, δ, a square aperture with sides of $D_N = \lambda f/\delta$ corresponds to the Nyquist sampling condition.[4] Apertures smaller than this lead to loss of information and high bit-error rate (BER); larger apertures produce less interpixel cross talk but provide lower density.

An optical system for high-density holographic data storage achieves a small Nyquist aperture by use of large SLM pixels and short-focal-length optics.[4,5] Since increasing the number of pixels in each data page does not change the minimum allowable aperture size, large data pages are desirable for high density (as well as a fast readout rate). However, large data pages increase the demands on the optical imaging system.

Once the optical system is configured to successfully pass the SLM data to the detector array despite the small aperture at the storage material, multiple holograms must still be recorded and retrieved independently. This adds two additional terms to the overall signal-to-noise budget: interpage cross talk caused by incomplete Bragg mismatch and the decrease in diffraction efficiency caused by sharing the finite dynamic range of the storage material among the superimposed holograms. In the 90° geometry in $LiNbO_3$, interpage cross talk is less important than the limited dynamic range. If M is the number of superimposed holograms, then the diffraction efficiency falls as $(M\#/M)^2$.[6] Here $M\#$ is a scaling coefficient that describes both system and material properties.[7] Achieving high areal density is then a balancing act between the interpixel cross talk introduced by the small aperture and the loss of signal associated with recording multiple holograms. Previously, high areal density (100 pixels/μm^2) was demonstrated when a relatively small number of pixels from superimposed data pages was sampled.[8] In contrast, pixel matching of large data pages was demonstrated only for a few holograms stored at low areal density (~0.35 pixels/μm^2).[9] In this Letter we demonstrate holographic storage of 1000 1-Mpixel data pages through a small transverse aperture, demonstrating a channel density of 394 pixels/μm^2. For comparison, a CD has a density of ~0.7 bits/μm^2; a DVD disk, ~4.5 bits/μm^2; and the magnetic disk in the 1-GB IBM MicroDrive, ~23 bits/μm^2.

The DEMON2 platform, shown in Fig. 1, was designed for high-density angle-multiplexed holographic storage using the 90° geometry. Light from a frequency-doubled diode-pumped Nd:YAG laser (λ = 532 nm) was expanded and split into reference and object beams. The object beam was apodized

0146-9592/01/070444-03$15.00/0

with a pair of aspherical optical elements, yielding illumination uniformity within 5% rms with 80% of the input optical power.[10] After apodization, the object beam was further expanded and directed through a polarizing beam splitter onto the surface of a 1024 × 1024 pixel liquid-crystal-on-silicon reflective SLM[12]. The pixel pitch was $\delta = 12.8\ \mu$m, and the areal fill factor was 88%. Custom optics (effective focal length $f = 30$ mm) imaged the SLM pattern through the $LiNbO_3$:Fe storage material (15 mm × 15 mm × 8 mm, c axis at 45° in the horizontal plane, 0.02% Fe-doped, $\alpha \sim 0.8\ \text{cm}^{-1}$) and onto the detector array (Dalsa CA-D4-1024). The detector pitch was 12 μm, with a fill factor of >90%, and the detected data page was pixel matched 1:1 over the entire 1024 × 1024 pixels. The camera frame rate was 40 Hz. A square aperture of 1.7 mm × 1.7 mm, placed directly at the Fourier-transform plane, was found to introduce a tolerable amount of interpixel cross talk (the Nyquist aperture for this system is 1.25 mm × 1.25 mm). The object beam entered the 15 mm × 15 mm face of the crystal 1.5 mm downstream from the aperture and centered 5 mm from the reference beam's orthogonal entrance face.

The reference beam was compressed vertically and apertured to a size of 5 mm wide by 1.9 mm tall. This collimated beam was directed by a galvanometric mirror deflector (Cambridge Instruments 602HC-6450) through a pair of scan lenses in a 4-F configuration and onto the 8 mm × 15 mm face of the crystal. Because the object beam diverged rapidly away from the Fourier-transform plane, we aligned the reference beam to meet the object beam immediately on entering the crystal. To prevent excessive scattering we covered this near corner of the crystal with a thin strip of black tape, placed a 4.5 mm × 4.5 mm aperture in the object beam 1 mm downstream from the crystal, and blocked the Fourier-transform aperture after hologram recording. The optical setup including laser occupied 0.8 m × 0.8 m.

After each hologram exposure, displacing the crystal both horizontally and vertically averaged out the BER degradation caused by the photovoltaic effect. This charge-transport process causes unidirectional displacement of the charge along the c axis, horizontally across the volume illuminated by the spatially nonuniform object beam.[7,12] Because of the amplitude-modulated SLM, half the power in the Fourier-transformed object beam is in the zero spatial-frequency component. Thus there are large intensity gradients at the boundary between the bright center component of the object beam and the dimmer outside portions. During recording, the photovoltaic effect conveys the charge from one of these vertical boundaries to the other, producing index changes through the electro-optic effect. Without movement of the crystal, this would eventually cause a severe BER distortion at localized portions of the received data page, especially in the final pages of the recording schedule.[6] When the crystal is continually displaced, however, the effect is averaged over the exposed volume of the crystal. This increases the maximum tolerable exposure time and modulation depth, improving the achievable M# and thus the number of holograms that can be superimposed.

However, this crystal motion implies that each stack of multiplexed holograms is partly exposed while neighboring stacks are recorded. To account for this experimentally, we spatially multiplexed 9 stacks of 1000 holograms each in the crystal, arranged over the object beam entrance face in a 3 × 3 grid on 1.6-mm centers. During the recording of each stack, the crystal was moved so that the optical axis of the object beam rastered within a 1.6 mm × 1.6 mm square on the crystal face. While the central column of three stacks was being recorded, the reference beam exposed all the stacks; the outer six stacks then received only object-beam exposure. This approach guaranteed that every hologram in the center stack received optical exposure corresponding to 1000 overlapping holograms, regardless of its relative position. Each stack was recorded with identical recording exposure schedules[6,7]: a last recording exposure of 0.21 s and an erasure time constant of 320 s. This sacrifices ~35% of the maximum potential M# (Ref. 7) to achieve an average recording exposure of 0.34 s. Most holograms were spaced in angle by 0.016°. However, to decrease the spatial overlap between holograms in different stacks but with similar reference-beam angles, one of these angle slots was skipped after every 10. With 6.2 mW in the object beam and 15.4 mW in the reference beam, this schedule produced an average diffraction efficiency of 1.1×10^{-6} or a realized M# of 1.07. With each hologram containing 1.01×10^6 raw pixels and an effective area A defined by stack spacing of 1.6 mm, the resulting areal density in channel bits was 394 pixels/μm^2 (254 Gpixels/in.^{2}).

After recording, we sampled 100 pages from the central stack with a readout power of 345 mW. Roughly half these pages were consciously chosen, either from the error-prone first 100 holograms or to provide coverage of the whole schedule; the remainder were

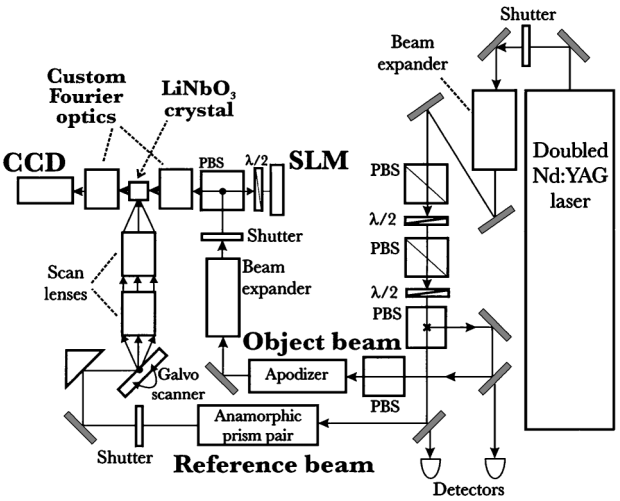

Fig. 1. DEMON2 holographic storage platform. An apodized beam uniformly illuminates a reflective SLM, which is then imaged to a matched CCD array through a small aperture by use of short-focal-length optics. PBS's, polarizing beam splitters; $\lambda/2$, half-wave plates.

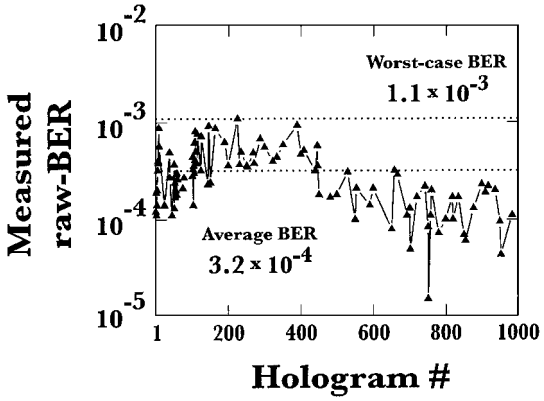

Fig. 2. Measured raw BER of retrieved holograms as a function of hologram number (position within the recording schedule).

randomly picked. For each, the crystal was translated to the position used to store that hologram. Postprocessing each retrieved page with a nonlinear equalization procedure[13] allowed us to compensate for the effects of both global misregistration and local pixel shifts (i.e., optical distortion). Approximately 40,000 pixels either were ignored completely (bad corner pixels or regions used for fiducial marks) or were remapped by use of a dedicated buffer on the data page. The 1,009,692 remaining pixels were modulation decoded with an 8-bits-in-12-pixels modulation code,[14] resulting in 670,816 raw data bits. The resulting raw BER for the retrieved holograms is shown in Fig. 2. Given the worst-case raw BER of 1.1×10^{-3}, an 8-bits-per-symbol Reed–Solomon error-correction code with a code rate of 0.92 could correct the raw BER to the desired user BER of 10^{-12}.[15,16] We made the simplistic assumption that raw byte errors can be uniformly distributed across the error-correction code code words through proper interleaving.[17] The overall system code rate of 0.61 leads to a storage density in user bits of 241.5 bits/μm^2 (155.8 Gbits/in.^{2}).

Given the ~5.5-mm stack thickness, the raw volumetric density achieved here is 0.072 pixels/μm^3. With $\lambda = 532$ nm, this corresponds to approximately 1.08% of $1/\lambda^3$. However, the DEMON2 optics supports a full angle of 25° in the object beam and 36° in the reference-beam optics. If we disregard all noise sources except those that are due to diffraction (interpage and interpixel cross talk), then the largest volumetric density theoretically supported by these optics is 11% of $1/\lambda^3$, achieved with 6500 holograms (first Bragg null) through a 1.25 mm × 1.25 mm aperture. To reach $1/\lambda^3$, both the reference and the object beams would have to approach a full angle of 90°. Even higher densities could possibly be realized by use of a cylindrical or spherical crystal to exploit fully the high index of refraction.

In conclusion, we have demonstrated high-areal-density holographic storage by confining the data-bearing object beam to a small aperture and by angle multiplexing a large number of holograms behind this aperture. Innovations include short-focal-length low-aberration optics, aspheric optics for beam apodization,[10] and a shift-compensation algorithm to relax distortion and alignment tolerances.[13] By superimposing 1000 holograms within an effective transverse area of 1.6 mm × 1.6 mm, we demonstrated a channel areal density of 394 pixels/μm^2 (254 Gpixels/in.^{2}). Volumetrically, this high density represents only 1.08% of the well-known theoretical limit of $1/\lambda^3$. Strong modulation codes,[14] together with conventional Reed–Solomon error-correction codes, delivered user data at $<10^{-12}$ BER with a 61% overall code rate. These results can be extended either to high capacity through a disk-based format[2,8] or to both high capacity and fast access through phase-conjugate readout of stationary crystalline media.[3,18]

G. W. Burr's e-mail address is burr@almaden.ibm.com.

References

1. P. J. van Heerden, Appl. Opt. **2,** 393 (1963).
2. D. Psaltis and F. Mok, Sci. Am. **273,** 70 (1995).
3. J. H. Hong, I. McMichael, T. Y. Chang, W. Christian, and E. G. Paek, Opt. Eng. **34,** 2193 (1995).
4. M.-P. Bernal, G. W. Burr, H. Coufal, and M. Quintanilla, Appl. Opt. **37,** 5377 (1998).
5. J. Ashley, M.-P. Bernal, G. W. Burr, H. Coufal, H. Guenther, J. A. Hoffnagle, C. M. Jefferson, B. Marcus, R. M. Macfarlane, R. M. Shelby, and G. T. Sincerbox, IBM J. Res. Dev. **44,** 341 (2000).
6. D. Psaltis, D. Brady, and K. Wagner, Appl. Opt. **27,** 1752 (1988).
7. F. H. Mok, G. W. Burr, and D. Psaltis, Opt. Lett. **21,** 896 (1996).
8. A. Pu and D. Psaltis, in *1997 Optical Data Storage Topical Meeting* (Institute of Electrical and Electronics Engineers, New York, 1997), pp. 48–49.
9. R. M. Shelby, J. A. Hoffnagle, G. W. Burr, C. M. Jefferson, M.-P. Bernal, H. Coufal, R. K. Grygier, H. Günther, R. M. Macfarlane, and G. T. Sincerbox, Opt. Lett. **22,** 1509 (1997).
10. J. A. Hoffnagle and C. M. Jefferson, Appl. Opt. **39,** 5488 (2000).
11. J. L. Sanford, P. F. Greier, K. H. Yang, M. Lu, R. S. Olyha, Jr., C. Narayan, J. A. Hoffnagle, P. M. Alt, and R. L. Melcher, IBM J. Res. Dev. **42,** 411 (1998).
12. A. M. Glass, D. von der Linde, and T. J. Negram, Appl. Phys. Lett. **25,** 233 (1974).
13. G. W. Burr and T. Weiss, "Compensation for pixel misregistration in volume holographic data storage," Opt. Lett. (to be published).
14. G. W. Burr, J. Ashley, H. Coufal, R. K. Grygier, J. A. Hoffnagle, C. M. Jefferson, and B. Marcus, Opt. Lett. **22,** 639 (1997).
15. I. S. Reed and G. Solomon, J. Soc. Ind. Appl. Math. **8,** 300 (1960).
16. G. W. Burr, W.-C. Chou, M. A. Neifeld, H. Coufal, J. A. Hoffnagle, and C. M. Jefferson, Appl. Opt. **37,** 6951 (1998).
17. W.-C. Chou and M. A. Neifeld, Appl. Opt. **37,** 6951 (1998).
18. G. W. Burr and I. Leyva, Opt. Lett. **25,** 499 (2000).